

**INFLUENCE OF LARGE-SCALE ANTARCTIC
OROGRAPHY AND ICE SHEETS ON ATMOSPHERIC
CIRCULATION AND ENERGY TRANSPORT**

KAMAL TEWARI



**DEPARTMENT OF APPLIED MECHANICS
INDIAN INSTITUTE OF TECHNOLOGY DELHI, NEW DELHI-110016
AUGUST 2022**

Influence of Large-Scale Antarctic Orography and Ice Sheets on Atmospheric Circulation and Energy Transport

by

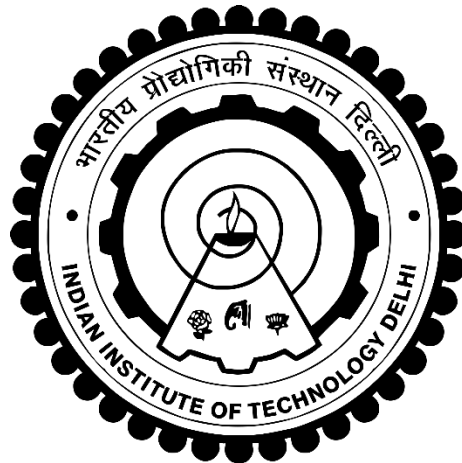
Kamal Tewari

(2017AMZ8119)

Department of Applied Mechanics

Submitted

In fulfilment of the requirements of the degree of Doctor of Philosophy



INDIAN INSTITUTE OF TECHNOLOGY DELHI, NEW DELHI-110016

AUGUST 2022

CERTIFICATE

This is to certify that the thesis entitled “**Influence of Large-Scale Antarctic Orography and Ice Sheets on Atmospheric Circulation and Energy Transport**” being submitted by **Mr. Kamal Tewari** is the report of bonafide research work carried out by him under our supervision. This thesis has been prepared in conformity with the rules and regulations on Indian Institute of Technology Delhi. We further certify that the thesis has attained a standard required for the award of **Doctor of Philosophy** degree of the Institute. The research reported and the results presented in the thesis have not been submitted, in part or full to any other institute or university for the award of any other degree or diploma.

Dr. Anupam Dewan
Professor
Department of Applied Mechanics
Indian Institute of Technology Delhi
Hauz Khas, New Delhi, Delhi – 110016

Dr. Saroj Kanta Mishra
Associate Professor
Center for Atmospheric Sciences
Indian Institute of Technology Delhi
Hauz Khas, New Delhi, Delhi – 110016

Date :

Place :

ACKNOWLEDGEMENTS

First and foremost, I would like to express my gratitude to my supervisors Prof. Anupam Dewan and Prof. Saroj Kanta Mishra for their constant support and guidance throughout the Ph.D. program. They had been very motivating, and I owe the success of my work to their encouragement and much-needed advice. Their sincerity, thoroughness, and perseverance have been a constant source of inspiration for me. They have played a very instrumental role in shaping my scientific aptitude over these years and have truly prepared me as a research scientist. Their trust and relentless encouragement have not only helped me to grow as an independent researcher but have also allowed me to develop skills to face any challenging situations. Their advice on both research as well as on my career has been invaluable.

Next, I would also like to express my gratitude to my research committee members, Prof. Sanjeev Sanghi, Prof. B. Premachandran, and Prof. Arjun Sharma, for providing valuable suggestions whenever needed. I would like to thank the entire faculty and staff members of the Applied Mechanics department for their assistance and cooperation during coursework and for making my Ph.D. work to be an enjoyable moment. I also thank Prof. Hisashi Ozawa for providing me an opportunity to work under him at Hiroshima University, Japan. I had an amazing learning experience during my stay and the discussions with him thereafter through my journey are invaluable. I would also like to thank my collaborators Dr. Mark England, Prof. Hansi Singh, Prof. In-Sik Kang, and Dr. John Fasullo for providing their valuable comments on various works.

I am grateful to my parents Mr. Jagdish Chandra Tewari, and Mrs. Anju Tewari, for embracing my Ph.D. journey and for providing me with moral and emotional supports through these years. I am grateful to my sister Ms. Garima Tewari for her constant love, support, and motivation. I am also thankful to my other family members and friends who have supported me along the way.

I believe this is an apt opportunity to express my gratitude towards all the persons who helped me directly or indirectly during this thesis work. I am thankful to Dr. Anuj K. Shukla, Dr. Popat Salunke, Dr. Sartaj Tanweer, Dr. Tej Pratap Singh, Dr. Abhishek Anand, Dr. Raju Pathak, Mr. Gaurav Dogra, Mr. Ashutosh Jaiswal, Mr. Prabhakar, Ms. Sweta Choubey, Mr. Pankaj, Mr. Mohit Garg, Mr. Yadwinder Singh Joshan, Mr. Kuldeep Yadav, Mr. Ranjeet and all my friends for their support and making my life enjoyable at IIT Delhi. Last but by no means least, I am also grateful to everyone in DST-CoE in Climate Modelling and CFD lab as it was an excellent experience to share the laboratory with all of you during my research. Thanks for all your encouragements. Further, I would like to express my special gratitude to JASSO and IIT Delhi for helping and providing the fellowships for the research work. I also thank DST-CoE in Climate Modelling, IIT Delhi for partially supporting this research.

Finally, I want to thank Almighty God for providing me strength, showing me the right path, and showering countless blessings on me, so that I have been finally able to accomplish my thesis.

Kamal Tewari

ABSTRACT

The effects of obstacles, such as, mountains and plateaus, on heat transfer and fluid flow in the earth's atmosphere have always been a subject of research due to their economic and environmental importance in shaping food production and the world's climate. They are one of the most stunning features of the landscape and play a major role in affecting the climatology of a particular location and thus determining its natural habitat. The flow of air, structure of clouds, surface evaporation, transport of heat and moisture through the atmosphere are all steered by their orographic effects. Mechanically, the surface orography acts as a flow barrier that forces the air to deflect, rise and cool, generate waves, and sometimes cause temperature inversion. Thermodynamically, these elevated terrains during summers act as the heat sources and cause instability due to surface heating. These thermo-mechanical effects of the orography influence the general circulation and energy transport in the planet.

Paleoclimate evidence suggests that the earth's orography has constantly been changing over a long-time scale. But in the present era, with the rapid changes in climate and global warming becoming more apparent worldwide, orographic changes due to ice melting and glaciers loss, especially over the polar regions, have accelerated. The Antarctic continent has undergone complex changes in the past few decades due to the human intervention, which raises concerns regarding the future of the largest cryosphere reserve on the planet. Despite this fact, the consequences of orographic change over the Antarctic have received little attention partly due to its long geographic isolation and non-decreasing sea ice trend compared to its northern counterpart. Under the projected trajectory of the greenhouse emissions, the climate of the continent is projected to become wetter, warmer, and more prone to ice sheet meltdown and sea ice loss. Consequently, the orography and ice cover are expected to fluctuate drastically in the future due to warming, which will exert feedback on the atmospheric circulation (mean flow and eddies). Detangling the effects of these changes on climate systems from other changes accompanied due to warming is required for a better understanding of their impact on the Polar climate. Therefore, the overreaching aim of the present thesis is to examine the influence of the large-scale Antarctic orography and ice sheets on the atmospheric circulation and energy transfer on the planet, using comprehensive climate models.

In the first half of the thesis, we use the atmospheric general circulation model to evaluate the role of Antarctic orography in the general circulation and energy transport on the planet. First,

the impact of Antarctic orographic suppression is presented to highlight the importance of its orography on the global climate. It is demonstrated that the reduction in Antarctic orography would enhance the poleward energy transport by causing changes in the mean atmospheric circulation and enhancement in the eddy motions over the Southern Hemisphere. Simulations performed by altering the orography further suggest that a reduction from the current orographic configuration will influence its local climate by changing the seasonal precipitation, causing tropospheric and surface warming, changes in winds, stationary waves, and energy transport over the region. Orographic enhancement is noted to cause the opposite response. These results suggest that although the Antarctic continent is geographically isolated from the rest of the world, it exerts climatic influence, which is experienced locally and globally through the changes in the stationary eddies, energy transport, and general circulation.

In the second half of the thesis, we use coupled atmosphere-ocean climate models to investigate the remote impact of Antarctic orography and its sea-ice extent on the global climate. Specifically, we study the teleconnections of the Antarctic ice sheet with the South Asian monsoon system, influencing the energy transport over the monsoon domain through atmosphere-ocean coupling. We examine the impact of Antarctic ice sheet reduction on monsoon circulation, precipitation, and energy transport. We demonstrate that the monsoon system is significantly strengthened by the Antarctic orographic reduction, specifically over the Southern Hemisphere, and this strengthening partly compensates for the excess poleward energy demand. Further, through the coupled sea-ice reduction modelling simulations, we examine the global influence of the projected sea ice loss and the associated mechanism on the climate system. The results indicate that, like the Antarctic orographic height, its sea ice cover also strongly influences the atmospheric circulation and energy transport on the planet. A reduction in its sea ice cover in the future will lead to a mini global warming signal and cause significant changes in the mean flow and eddies over the Southern Hemisphere, thereby reducing the poleward energy transport. These results highlight the intimate coupling of the Antarctic orography and its sea ice cover with the global climate and demonstrate the importance of its orographic presence besides its direct contribution to the rising sea levels.

सारांश

पृथ्वी के वायुमंडल में गर्मी हस्तांतरण और द्रव प्रवाह पर बाधाओं, जैसे पहाड़ों और पठारों के प्रभाव, खाद्य उत्पादन और दुनिया की जलवायु को आकार देने में उनके आर्थिक और पर्यावरणीय महत्व के कारण हमेशा शोध का विषय रहा है। वे परिदृश्य की सबसे आश्चर्यजनक विशेषताओं में से एक हैं और किसी स्थान के जलवायु विज्ञान को प्रभावित करने और इस प्रकार इसके प्राकृतिक आवास का निर्धारण करने में एक प्रमुख भूमिका निभाते हैं। वायु का प्रवाह, बादलों की संरचना, सतह का वाष्पीकरण, वातावरण के माध्यम से गर्मी और नमी का परिवहन, सभी उनके भौगोलिक प्रभाव से प्रभावित होते हैं। यंत्रवत् रूप से, सतह की ऑरोग्राफी एक प्रवाह अवरोधक के रूप में कार्य करती है जो हवा को विक्षेपित करने, उठाने और ठंडा करने, तरंगों को उत्पन्न करने और कभी-कभी तापमान को व्युत्क्रम करने का कारण बनती है। ऊष्मागतिकीय रूप से, ग्रीष्मकाल के दौरान ये ऊंचे इलाके गर्मी के स्रोत के रूप में कार्य करते हैं और सतह के गर्म होने के कारण अस्थिरता पैदा करते हैं। ऑरोग्राफी के ये थर्मो-मैकेनिकल प्रभाव ग्रह में सामान्य परिसंचरण और ऊर्जा परिवहन को प्रभावित करते हैं।

पुरापाषाणकालीन साक्ष्य बताते हैं कि लंबे समय के पैमाने पर पृथ्वी की रूपरेखा लगातार बदल रही है। लेकिन वर्तमान युग में, दुनिया भर में जलवायु में तेजी से बदलाव और ग्लोबल वार्मिंग के अधिक स्पष्ट होने के साथ, बर्फ के पिघलने और ग्लेशियरों के नुकसान के कारण भौगोलिक परिवर्तन, विशेष रूप से ध्रुवीय क्षेत्रों में तेज हो गए हैं। मानव हस्तक्षेप के कारण पिछले कुछ दशकों में अंटार्कटिक महाद्वीप में जटिल परिवर्तन हुए हैं, जो ग्रह पर सबसे बड़े क्रायोस्फीयर रिजर्व के भविष्य के बारे में चिंता पैदा करता है। इस तथ्य के बावजूद, अंटार्कटिक पर भौगोलिक परिवर्तन के परिणामों पर इसके उत्तरी समकक्ष की तुलना में इसके लंबे भौगोलिक अलगाव और गैर-घटती समुद्री बर्फ की प्रवृत्ति के कारण आंशिक रूप से थोड़ा ध्यान दिया गया है। ग्रीनहाउस उत्सर्जन के अनुमानित प्रक्षेपवक्र के तहत, महाद्वीप की जलवायु में नमी, गर्मी आने का और बर्फ की चादर के पिघलने और समुद्री बर्फ के नुकसान होने का अनुमान है। नतीजतन, अंटार्कटिक ऑरोग्राफी और आइस कवर में वार्मिंग के कारण भविष्य में भारी उतार-चढ़ाव की उम्मीद है, जो वायुमंडलीय परिसंचरण (औसत प्रवाह और इडिएस) पर प्रतिक्रिया व्यक्त करेगा। वार्मिंग के कारण होने वाले अन्य परिवर्तनों से जलवायु प्रणालियों पर इन परिवर्तनों के प्रभावों का पता लगाना, ध्रुवीय जलवायु पर उनके प्रभाव की बेहतर समझ के लिए आवश्यक है। इसलिए, इस थीसिस का व्यापक उद्देश्य विस्तृत जलवायु मॉडल का उपयोग करके ग्रह पर वायुमंडलीय परिसंचरण और ऊर्जा हस्तांतरण पर बड़े पैमाने पर अंटार्कटिक ऑरोग्राफी और आइस शीट के प्रभाव की जांच करना है।

थीसिस की पहली छमाही में, हम ग्रह पर सामान्य परिसंचरण और ऊर्जा परिवहन में अंटार्कटिक ऑरोग्राफी की भूमिका का मूल्यांकन करने के लिए वायुमंडलीय सामान्य परिसंचरण मॉडल का उपयोग करते हैं। सबसे पहले, अंटार्कटिक भौगोलिक दमन के प्रभाव को वैश्विक जलवायु पर इसकी रूपरेखा के महत्व को उजागर करने के लिए प्रस्तुत किया गया है। यह प्रदर्शित किया गया है कि अंटार्कटिक ऑरोग्राफी में कमी से दक्षिणी गोलार्ध में औसत वायुमंडलीय परिसंचरण में परिवर्तन और एडी गति में वृद्धि के कारण ध्रुवीय ऊर्जा परिवहन में वृद्धि होगी। ओरोग्राफिक में परिवर्तन करके किये गए सिमुलेशन आगे बताते हैं कि वर्तमान भौगोलिक विन्यास में परिवर्तन मौसमी वर्षा को बदलकर इसकी स्थानीय जलवायु को प्रभावित करेंगे, जिससे क्षोभमंडल और सतह के गर्म होने, हवाओं में परिवर्तन, स्थिर तरंगों और क्षेत्र में ऊर्जा परिवहन हो सकता है। ऑरोग्राफिक एन्हांसमेंट करने से विपरीत प्रतिक्रिया प्राप्त होगी। इन परिणामों से पता चलता है कि हालांकि अंटार्कटिक महाद्वीप भौगोलिक रूप से दुनिया के बाकी हिस्सों से अलग-थलग है, लेकिन यह जलवायु प्रभाव डालता है, जिसे स्थानीय और विश्व स्तर पर स्थिर एडी, ऊर्जा परिवहन और सामान्य परिसंचरण में परिवर्तन के माध्यम से अनुभव किया जाता है।

थीसिस के दूसरे भाग में, हम अंटार्कटिक ऑरोग्राफी और वैश्विक जलवायु पर इसकी समुद्री बर्फ की सीमा के दूरस्थ प्रभाव की जांच करने के लिए युग्मित वातावरण-महासागर जलवायु मॉडल का उपयोग करते हैं। विशेष रूप से, हम दक्षिण एशियाई मानसून प्रणाली के साथ अंटार्कटिक बर्फ की चादर के टेलीकनेक्शन का अध्ययन करते हैं, जो वायुमंडल-महासागर युग्मन के माध्यम से मानसून डोमेन पर ऊर्जा परिवहन को प्रभावित करते हैं। हम मानसून परिसंचरण, वर्षा और ऊर्जा परिवहन पर अंटार्कटिक बर्फ की चादर में कमी के प्रभाव की जांच करते हैं। हम प्रदर्शित करते हैं कि विशेष रूप से दक्षिणी गोलार्ध में अंटार्कटिक भौगोलिक कमी से मानसून प्रणाली काफी मजबूत होती है, और यह मजबूती आंशिक रूप से अतिरिक्त ध्रुवीय ऊर्जा मांग के लिए क्षतिपूर्ति करती है। इसके बाद, युग्मित समुद्री-बर्फ में कमी मॉडलिंग सिमुलेशन के माध्यम से, हम अनुमानित समुद्री बर्फ के नुकसान और जलवायु प्रणाली पर संबंधित तंत्र के वैश्विक प्रभाव की जांच करते हैं। परिणामों से संकेत मिलता है कि, अंटार्कटिक भौगोलिक ऊंचाई की तरह, इसका समुद्री बर्फ का आवरण भी ग्रह पर वायुमंडलीय परिसंचरण और ऊर्जा परिवहन को दृढ़ता से प्रभावित करता है। भविष्य में इसके समुद्री बर्फ के आवरण में कमी से एक मिनी ग्लोबल वार्मिंग संकेत मिलेगा और दक्षिणी गोलार्ध में औसत प्रवाह और एडी में महत्वपूर्ण परिवर्तन होंगे, जिससे ध्रुवीय ऊर्जा परिवहन कम हो जाएगा। ये परिणाम वैश्विक जलवायु के साथ अंटार्कटिक ऑरोग्राफी और इसके समुद्री बर्फ के आवरण के अंतरंग युग्मन को उजागर करते हैं और बढ़ते समुद्र के स्तर में इसके प्रत्यक्ष योगदान के अलावा इसकी भौगोलिक उपस्थिति के महत्व को प्रदर्शित करते हैं।

TABLE OF CONTENTS

| | |
|---|-------------|
| CERTIFICATE..... | i |
| ACKNOWLEDGEMENTS | iii |
| ABSTRACT..... | v |
| LIST OF FIGURES | xi |
| LIST OF TABLES | xvii |
| NOMENCLATURE..... | xix |
| 1.INTRODUCTION | 1 |
| 1.1 Introduction and Motivation..... | 2 |
| 1.2 Background..... | 5 |
| 1.3 Atmospheric Circulation, Energy Transport and the Antarctic Orography..... | 8 |
| 1.4 Objectives and Scope of Present Thesis..... | 18 |
| 1.5 Layout of Present Thesis | 19 |
| 2.GOVERNING EQUATIONS AND COMPUTATIONAL METHODOLOGY | 20 |
| 2.1 Atmospheric Flows and their Modelling Strategies | 21 |
| 2.2 Modelling Approaches Used | 25 |
| 2.3 Model Selection and Simulation Details | 29 |
| 3.EFFECTS OF THE ANTARCTIC ELEVATION ON THE ATMOSPHERIC CIRCULATION | 37 |
| 3.1 Introduction | 38 |
| 3.2 Data and Methodology | 40 |
| 3.3 Results and Discussion | 42 |
| 3.4 Summary..... | 55 |
| 4.INFLUENCE OF THE HEIGHT OF THE ANTARCTIC ICE SHEET ON ITS REGIONAL CLIMATE | 57 |
| 4.1 Introduction | 58 |
| 4.2 Data and Methodology | 60 |
| 4.3 Results and Discussion | 61 |
| 4.4 Summary..... | 74 |

| | |
|--|------------|
| 5. TELECONNECTIONS OF ANTARCTIC ICE SHEET WITH THE SOUTH ASIAN MONSOON | 76 |
| 5.1 Introduction | 77 |
| 5.2 Data and Methodology | 78 |
| 5.3 Results and Discussion | 79 |
| 5.4 Summary..... | 86 |
| 6. EFFECTS OF PROJECTED ANTARCTIC SEA ICE LOSS ON THE CLIMATE SYSTEM..... | 88 |
| 6.1 Introduction | 89 |
| 6.2 Data and Methodology | 91 |
| 6.3 Results and Discussion | 93 |
| 6.4 Summary..... | 102 |
| 7. CONCLUSIONS | 105 |
| REFERENCES..... | 109 |
| Appendix..... | 120 |
| A) RESPONSE OF THE ATMOSPHERE TO OROGRAPHIC FORCINGS: INSIGHTS FROM AQUAPLANET SIMULATIONS..... | 120 |
| a.1 Introduction..... | 121 |
| a.2 Data and Methodology..... | 123 |
| a.3 Results and Discussion | 126 |
| a.4 Summary..... | 144 |
| PUBLICATIONS FROM THE THESIS | 146 |
| BRIEF BIO-DATA OF AUTHOR | 147 |

LIST OF FIGURES

Figure 1.1: Schematic depiction of the surface winds and other features in the atmospheric circulation patterns over an idealized aquaplanet with the sun directly overhead at the equator (left) and the actual Earth (right).....**10**

Figure 1.2: Decomposition of the meridional energy transport obtained from the CESM control run into a) Atmospheric and oceanic transport b) Latent energy (LE) and Dry static energy (DSE) transport, and c) corresponding mean and eddy components.....**14**

Figure 1.3: Antarctic orography in meters above the sea level and the various sectors.**16**

Figure 1.4: Antarctic sea-ice extent anomaly in the past four decades (scaled by 10^6 km²) computed with respect to the 1981-2010 average (Data Source: National Snow and Ice Data Center). The solid line indicates the 12-months running average, while the red line indicates the overall trend.**17**

Figure 2.1: Categorization of the climate models in terms of complexity as in Bony et al. (2013)...**22**

Figure 2.2: An aquaplanet simulation from the Nonhydrostatic Icosahedral Atmospheric Model**26**

Figure 2.3: Schematic illustration of the model grid used in atmospheric general circulation models. Source: The COMET Program.....**27**

Figure 2.4: Schematic structure of an Atmospheric Ocean general circulation model.....**28**

Figure 2.5: Scatter plot of Pattern Correlation Coefficient (PCC) versus (a) normalized Standard Deviation (NSD), (b) normalized Root Mean Square Error (NRMSE), and (c) box plot for annual mean snowfall over Antarctica in various CMIP5 models.....**30**

Figure 2.6: Schematic representation of CESM1.2, the various components of the model are, CAM: Community Atmosphere Model, CLM: Community Land Model, CICE: Sea Ice Model, DOCN: Data Ocean Model, and CPL: Coupler.....**33**

Figure 3.1: Topography (m) in the CTRL and EXPT simulations.**41**

Figure 3.2: Spatial distribution of changes in climatic variables (a) Surface temperature (K) (b) Sea level pressure (hPa) (c) Precipitation (mm day⁻¹) (d) Evaporation (mm day⁻¹) (e) Zonally averaged air temperature (K) with coloured lines representing the tropopause (2 K km^{-1} lapse rate contour) (f) Zonally averaged Specific humidity (g/kg) due to Antarctic orographic reduction expressed as EXPT-CTRL.**43**

Figure 3.3: Spatial distribution of change in energy flux (in Wm^{-2}) (a) Outgoing longwave (b) Absorbed short wave (c) Net incoming radiation at the top of the atmosphere (d) Zonally averaged

| | |
|--|----|
| changes in radiational fluxes due to Antarctic orographic reduction expressed as EXPT-CTRL. | 45 |
| Figure 3.4: Northward energy transport anomaly (in PW) due to Antarctic orographic reduction expressed as EXPT-CTRL (a) Total, atmospheric (Atm) and oceanic transport (Ocn) (b) Breakdown of northward atmospheric energy transport into Latent energy (LE) and Dry static energy (DSE) transport..... | 46 |
| Figure 3.5: Spatial distribution of Horizontal wind velocity and its anomaly (in ms^{-1}) at 850 hPa (a, b) and 200 hPa (c, d) plotted for latitudes beyond 60° S. The spatial contour in the figure shows mean wind vector speed and the biases in wind speed for the bias figures. Wind vector length measures wind speed (m/s). | 48 |
| Figure 3.6: Latitude – height plot of annual and zonally averaged response of Antarctic orographic reduction on winds and momentum flux: (a) Zonally averaged vertical winds for meridional circulation, representing the three cells of the atmospheric circulation and vectors showing vertical velocity anomaly (in ms^{-1}) (b) Zonal winds (ms^{-1}) and (c) Eddy momentum flux (m^2s^{-2}) in EXPT-CTRL runs. The color tone depicts the anomaly while the contours depict the mean state in CTRL run..... | 49 |
| Figure 3.7: Contours of changes in (a) Transient Eddy Kinetic Energy (m^2s^{-2}) (b) Normalized Available Potential Energy (APE) obtained in EXPT-CTRL. | 51 |
| Figure 3.8: Breakdown of northward dry and latent energy transport (in PW) into mean and eddy transport components (PW) (a) Absolute latent energy transport (b) Latent energy transport anomaly (c) Absolute dry static energy transport (d) Dry static energy transport anomaly. | 53 |
| Figure 3.9: Normalized meridional profile of the zonal and vertical mean values of the (a) Total (b) Mean (c) Transient eddy and (c) Stationary eddy component of the kinetic energy in m^2s^{-2} and the corresponding percentage change in these as observed in EXPT with respect to CTRL (e-h). ... | 54 |
| Figure 3.10: Schematic of the global atmospheric response to Antarctic orographic reduction (a) CTRL case representing the annual mean circulation and energy transport mechanism by mean flow and ocean (b) Modified circulation pattern with changes in energy transfer indicated by black arrows. | 55 |
| Figure 4.1: Antarctic topography as represented by the model simulations in meters (column 1: CTRL) and its corresponding anomalies plotted for latitudes beyond 60° S in various experiments. | 60 |
| Figure 4.2: Spatial distribution of the annual mean surface temperature (in K) over Antarctica (column 1: CTRL) and its corresponding anomalies plotted for latitudes beyond 60° S in various experiments. | 61 |

| | |
|---|-----------|
| Figure 4.3: Spatial distribution of annual mean precipitation (in mm/day) over Antarctica (column 1: CTRL) and its corresponding anomalies plotted for latitudes beyond 60° S in various experiments. | 62 |
| Figure 4.4: Multiyear (a) mean snowfall rate over Antarctica (in mm/year) and monthly mean snowfall variation (in mm/day) over (b) whole Antarctica and its two sectors namely (c) western and (d) eastern Antarctica in various AIS reduction simulations. | 65 |
| Figure 4.5: Same as Figure 4.4 but for AIS enhancement simulations..... | 66 |
| Figure 4.6: Annual mean lower-level wind circulation at 850 hPa over Antarctica (column 1: CTRL) and its corresponding anomalies plotted for latitudes beyond 60° S in various experiments. The vector length scales with the wind velocity..... | 68 |
| Figure 4.7: Annual mean upper-level wind circulation at 200 hPa over Antarctica (column 1: CTRL) and its corresponding anomalies plotted for latitudes beyond 60° S in various experiments. The vector length scales with the wind velocity..... | 69 |
| Figure 4.8: Contours of eddy stream function at 200 mb (scaled by $10^7 \text{ m}^2\text{s}^{-1}$) over Antarctica (column 1: CTRL) and its corresponding anomalies in various experiments plotted for Southern Hemisphere..... | 70 |
| Figure 4.9: Zonally averaged changes in the radiative fluxes (in Wm^{-2}) at the top of the atmosphere due to Antarctic orographic perturbation expressed as EXPT-CTRL in various experiments. Blue line represents the OLR, red line ASW and the green line the net downwelling radiative imbalance at the top of the atmosphere, respectively. | 72 |
| Figure 4.10: Changes in northward energy transport (in PW), zonally averaged over the (a) Ocean, (b) Atmosphere and (c) Total (a+b) due to AIS thickness perturbation expressed as EXPT-CTRL in various experiment. | 73 |
| Figure 5.1: (a) Surface temperature (K), (c) sea-level pressure (hPa), and (b,d) their corresponding anomalies in EXPT with respect to CTRL during JJAS. The monsoonal longitudes have been highlighted with blue colours in panel a, and the wind vectors depicting the low-level winds and their anomalies at 850 hPa have been superimposed on the sea-level pressure in panel c, d respectively..... | 80 |
| Figure 5.2: (a) Precipitation (P), (c) evaporation (E), (e) moisture convergence (P-E), and (b,d,f) their corresponding anomalies ($\text{mm}\cdot\text{day}^{-1}$) in EXPT with respect to CTRL during JJAS. The monsoonal longitudes have been highlighted with blue colours in panel a. | 82 |
| Figure 5.3: (a,b) Sector mean (70°–110°E) cross-section of the mass stream function and its anomaly (in $\text{Tg}\cdot\text{s}^{-1}$). (c,d) Meridional profile of northward energy transport in total, respective contribution | |

by the atmosphere, ocean and their corresponding anomalies (in PW). (e,f) Meridional profile of the radiation balance at the top of the atmosphere and its corresponding anomalies (in $W \cdot m^{-2}$). (g,h) Meridional profile of the radiation balance and turbulent fluxes at the surface and their corresponding anomalies (in $W \cdot m^{-2}$) as observed in EXPT with respect to CTRL during JJAS.

.....84

Figure 5.4: A schematic representation of the atmospheric response to Antarctic orographic reduction during summers (JJAS) observed over the monsoon domain. (a) CTRL case represents the global mean atmospheric circulation through the Hadley (H), Ferrel (F), and Polar (P) cells over the monsoon domain, (b) Modified circulation pattern with changes in the strength of the global circulation represented by the thickness of arrows.....86

Figure 6.1: (a) Spatial distribution of changes in sea ice fraction in EXPT with respect to CTRL plotted for latitudes beyond 45° S and (b) the seasonal cycle of Sea Ice Extent (SIE) in the two experiments over the Southern Hemisphere.....92

Figure 6.2: Spatial distribution of changes in climatic variables: (a) surface temperature (K), (b) precipitation ($mm \text{ day}^{-1}$), (c) evaporation ($mm \text{ day}^{-1}$), and (d) total cloud fraction due to Antarctic SIE reduction expressed as EXPT-CTRL.93

Figure 6.3: Latitude - height plot of annual response of Antarctic SIE reduction on: (a) zonally averaged air temperature (K), (b) zonally averaged specific humidity ($g \text{ kg}^{-1}$), and (c) zonally averaged vertical winds (in ms^{-1}) in EXPT-CTRL runs. In Figure 6.3c, the vectors shows the vertical velocity anomaly (scaled up by 100), contours depict the mean state in CTRL run, while the color tone indicates the changes in the mean meridional circulation (blue indicates rising motion and red indicates sinking motion).95

Figure 6.4: Spatial distribution of horizontal winds and its anomaly (in ms^{-1}) at 850 hPa (a, b) and 200 hPa (c, d) plotted for latitudes beyond 45° S. The colour bars in the figure show mean wind speed in CTRL and its differences for the anomalies. Wind vector length measures wind speed.....97

Figure 6.5: Annual mean Latitude-Height distributions of (a) zonal winds (ms^{-1}), (b) eddy momentum flux ($m^2 \text{ s}^{-2}$), and (c) transient eddy Kinetic energy ($m^2 \text{ s}^{-2}$), in EXPT-CTRL. The color tone depicts the anomaly, while the contours depict the mean state in the CTRL run.98

Figure 6.6: Zonally averaged changes in radiation fluxes (a) OLR, ASW and the net incoming radiation at the top of the atmosphere, (b) net upward longwave radiation (LW), net absorbed shortwave radiation (SW), upward sensible heat flux (SH), upward latent heat flux (LH), and net downward energy flux at the surface due to Antarctic SIE reduction expressed as EXPT-CTRL.99

Figure 6.7: Northward energy transport anomaly (in PW) due to Antarctic SIE reduction expressed as EXPT-CTRL: (a) total (Net), atmospheric (Atm), and oceanic transport (Ocn), (b) breakdown of northward atmospheric energy transport into latent energy (LE) and dry static energy (DSE) transport..... **100**

Figure 6.8: Breakdown of northward dry and latent energy transport (in PW) into mean and eddy transport components (PW): (a) absolute latent energy transport, (b) latent energy transport anomaly, (c) absolute dry static energy transport, and (d) dry static energy transport anomaly. **102**

Figure 6.9: Schematic of the global atmospheric response to Antarctic SIE reduction: (a) CTRL case representing the annual mean circulation, eddies and the energy transport mechanism by mean flow and ocean and (b) modified circulation pattern, in which the changes in strength of the mean circulation and eddies are represented by changes in thickness of arrows and the changes in energy transfer indicated by black arrows..... **103**

LIST OF TABLES

| | |
|---|-----------|
| Table 2.1 List of CMIP5 models used in the present study. | 31 |
|---|-----------|

NOMENCLATURE

| | |
|------------|--|
| T | Temperature |
| q | Specific humidity |
| p | Pressure |
| u_i | Velocity vector |
| x, y, z | Coordinate directions |
| f | Coriolis parameter |
| c_p | Specific heat at constant pressure |
| R | Gas constant |
| E, P | Evaporation and precipitation rate |
| H | Net convective and radiative heating |
| F_x, F_y | Parameterized components of the drag force |

Greek Symbols

| | |
|-----------|------------------------------------|
| τ | Time scale of averaging in seconds |
| λ | Longitude |
| ϕ | Latitude |
| ξ | Relative Vorticity |
| ω | Vertical Pressure Velocity |
| ψ | Stream function |
| ρ | Density |
| Ω | Angular speed of earth's rotation |

Superscript

| | |
|---|------------------------------|
| ' | Fluctuating quantity in time |
|---|------------------------------|

| | |
|-----|-------------------------------|
| * | Fluctuating quantity in space |
| - | Time averaged quantity |
| [] | Zonally averaged quantity |

Abbreviation

| | |
|-------|---|
| ACC | Antarctic Circumpolar Current |
| AIS | Antarctic Ice Sheet |
| AMIP | Atmospheric Model Intercomparison Project |
| AGCM | Atmospheric General Circulation Models |
| AOGCM | Atmospheric Ocean General Circulation Model |
| APE | Available Potential Energy |
| ASW | Absorbed Short Wave |
| CFD | Computational Fluid Dynamics |
| CAM5 | Community Atmosphere Model Version-5 |
| CESM | Community Earth System Model |
| CICE | Community Ice Code |
| CISM | CESM Land Ice Model |
| CLM | Community Land Model |
| CMIP | Coupled Model Intercomparison Project |
| CPL | Coupler |
| DNS | Direct Numerical Simulations |
| DOCN | Data Ocean Model |
| DSE | Dry Static Energy |
| EDSE | Eddy Dry Static Energy |

| | |
|---------|---|
| ELE | Eddy Latent Energy |
| ERA-I | ECMWF Reanalysis Interim |
| ESM | Earth System Model |
| GCM | Global Climate Model |
| GFD | Geophysical Fluid Dynamics |
| HadISST | Hadley Centre Sea-Ice and SST |
| IPCC | Intergovernmental Panel on Climate Change |
| ITCZ | Inter-tropical Convergence Zone |
| JJAS | June-July-August-September |
| LE | Latent Energy |
| LES | Large Eddy Simulations |
| MDSE | Mean Dry Static Energy |
| MJO | Madden Julian Oscillations |
| MLE | Mean Latent Energy |
| NCAR | National Center for Atmospheric Research |
| NH | Northern Hemisphere |
| NSD | Normalized Standard Deviation |
| NRMSE | Normalized Root Mean Square Error |
| OLR | Outgoing Longwave Radiation |
| PCC | Pattern Correlation Coefficient |
| POP2 | Parallel Ocean Program version 2 |
| RCP | Representative Concentration Pathway |
| RMSE | Root Mean Square Error |

| | |
|--------|--|
| SE | Stationary Eddy |
| SH | Southern Hemisphere |
| SIE | Sea Ice Extent |
| SLP | Sea Level Pressure |
| SST | Sea Surface Temperature |
| TAM | Transantarctic Mountains |
| TOA | Top of the Atmosphere |
| USGS | United States Geological Survey |
| WACCM4 | Whole Atmosphere Community Climate Model Version-4 |